Chapter 7
Evaluation of Injection-Molding Phenomena
Part 2: Measurement of flow and deformation of polymer under molding

1. Deformation Behavior of Polymer Materials: Viscoelasticity

In general, polymeric materials used in the forming processes including injection-molding show somewhat peculiar behavior under deformation, since the molecule has extremely long backbone. That is the "viscoelasiticity." All the materials are more or less viscoelastic, but the polymeric materials show clear viscoelasticity in the time range of our daily life, i.e. time in the range from several milliseconds to several hours, and the viscoelasticity strongly depends on their temperature.

Deformation behavior of the viscoelastic materials can be modeled most simply with combinations of one spring (elastic element) and one dashpot (viscous element) as shown in Figure 7.9. In these models, if contribution of the spring to deformation is dominant the material behaves as an elastic body, and the material becomes viscous if the dashpot is dominant. Since the effect of dashpot depends on its deformation rate while the force generated in the spring is independent on the deformation rate, deformation behavior of viscoelastic body depends upon time required for the deformation. Namely, viscoelastic bodies behave elastic if the deformation rate is high, and are viscous for slow deformation. This property of the viscoelastic bodies can be evaluated by the "characteristic time" of the materials. For example, the characteristic time of water is in order of picosecond, and thus water, which is usually a viscous liquid, behaves as an elastic body for deformation within the time-scale of picoseconds or less.

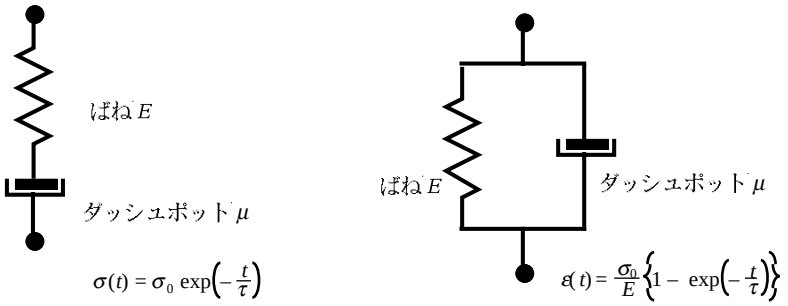

Figure 7.9 Simple models of viscoelastic materials:
Maxwell model (left) and Voigt Model (right).

Generally speaking, the characteristic time of thermoplastic polymers used in the molding process is in order of 10^6 seconds or more under the room temperature condition, but it rapidly decreases with temperature and becomes less than 1 second if the polymer is melted. This is the reason why the most of all molding processes of thermoplastic polymers have the stage for melting materials. In order to form a material into a prescribed shape, it is essential that the plastic deformation or flow in the materials take place. If not, the formed materials partially recover the original shape of raw materials due to elastic deformation. One of the objectives of the melting stage in the polymer processing is therefore to make the materials "forget" their original shape even if the time-scale of deformation due to molding is quite short, e.g. less than 1 second.

It is desirable to understand fully the viscoelasticity of materials for examining the flow and deformation behaviors polymer under the molding process.

2. Visualization of Flow and Stress Distribution in an Injection-Molded Polymer

Deformation behavior of the injection-molded polymer cannot be observed without using special devices because the molding of polymer takes place within the cavity of the mold usually made with metals. Indeed observation of flow of the polymer melt within the mold cavity can be achieved by using a mold having a window, e.g. Figure 7.10, and there have been many reports concerning the visualization results of polymer melt flow in the mold cavity. But information obtainable through these studies is limited since only the deformation of the material can be examined.

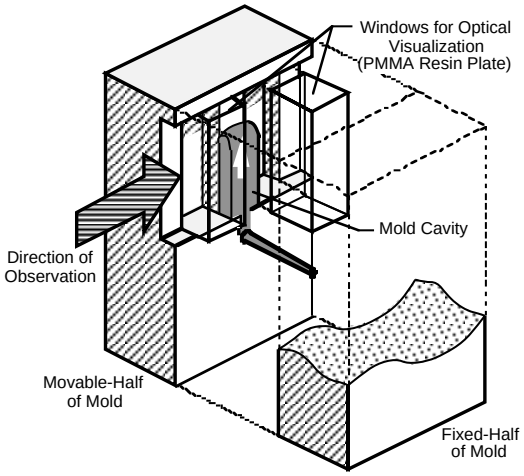

Figure 7.10 Visualization mold.

In order to discuss the deformation behavior of polymer under molding process from the viewpoint of viscoelasticity, information not only about the deformation but also about the stress induced in the polymer due to the deformation must be obtained through visualization. Visualization of stress distribution within a material can be most easily done by applying the method so-called photo-elasticity, which is often used in the field of strength of materials. In the photo-elasticity, stress in an optically transparent material is measured as the nonisotropy of the refraction index, i.e. birefringence, of material induced by the stress. The relation between the birefringence and stress is expressed by the Brewster's law as follows:

$$\Delta n = C(\sigma_1 - \sigma_2) \tag{7.3}$$

where Δn the birefringence observed, (σ_1 - σ_2) the principal stress difference in the material, and C the stress-optical coefficient depending the material. When stress distribution within a material is visualized by using the photo-elasticity, one can observe two types of fringes, one of them is a so-called isochromatic fringe and the other is an isoclinic fringe. The former corresponds the magnitude of principal stress difference in the material, and the latter is related to the direction of principal stress. Because determination of the direction of principal stress from the isoclinic fringes is time-consuming process, time-dependent stress field within a material is usually visualized by using the isochromatic fringes.

Figure 7.11 shows the optical setup for visualizing only the isochromatic fringes. This optical setup consists of a pair of polarizing plates (a polarizer and an analyzer), a pair of 1/4-wavelength plates for eliminating the isoclinic fringes, a monochromatic light source, and a camera for capturing the observed fringes. Using this optical setup, one can observe the rotation of polarizing plane due to birefringence within the material as the change of brightness of the light. Difference of birefringence $\Delta(\Delta n)$ between two positions correspond to the neighboring two fringes can be evaluated as

$$\Delta(\Delta n) \cdot W = \lambda \tag{7.4}$$

where W the optical path length of the object, and λ the wavelength of the light. Combining Eqs.

(7.3) and (7.4), one can evaluate the stress distribution within the object.

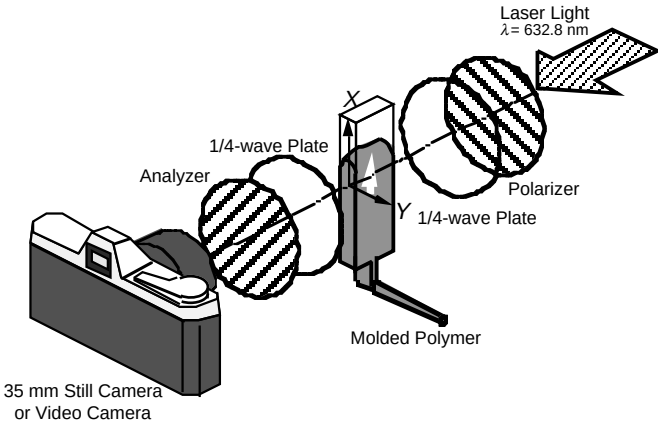

Figure 7.11 Optical setup for visualizing the isochromatic fringes.

The photo-elasticity can be applied also for visualizing stress distribution within the polymer under molding, if the polymer material is optically transparent. In this case, however, one should pay attention to that the stress-optical coefficient C is not constant in the polymer material. In general, the model for photo-elasticity used in the field of strength of materials is a solid at room temperature, and thus the stress-optical coefficient is considered to be uniform within the model. To the contrary, the stress-optical coefficient in injection-molded polymers is not uniform, and its distribution depends upon the time elapsed. Injection-molded polymer melt is cooled due to heat transfer to the mold wall, and solidifies gradually. Generation mechanisms of the birefringence in the solid polymer and in the polymer melt are different from each other, and thus the stress-optical coefficients of the solid and the melt are not identical[3)]. Therefore evaluation of stress distributions from the birefringence patterns observed in the injection-molded polymer requires more complicated procedure than that in the model at uniform temperature.

Figure 7.12 shows the successive photos[4)] of the isochromatic fringes observed in an injection-molded polymer by using the visualizing mold shown in Figure 7.10 and the optical setup of Figure 7.11. As shown in this figure, many almost parallel fringes with uniform spacing are observed in the polymer during the filling stage (Figure 7.11(a)). These fringes correspond to the distribution of shear stress induced due to polymer melt flow, since almost whole polymer in the mold is still molten and the stress-optical coefficient can be supposed to be uniform. Just after the whole cavity of the mold is filled with the polymer, the fringes disappear because the polymer flow stops (Figure 7.11(b)). The disappearance or relaxation of birefringence takes a certain time; in the case shown in Figure 7.11, it was about 0.2 second. This time corresponds to the characteristic time of the polymer. Careful inspection of Figure 7.11(b) shows that birefringence is remaining in thin regions adjacent to the mold wall while it disappears in the core region. This is because the polymer in these regions is cooled during the filling stage, and the characteristic time becomes longer than in the core region. As mentioned above, characteristic time of polymer strongly depends on its temperature, and become extremely long when the polymer solidifies. After that, birefringence pattern in the polymer slowly changes as shown in Figures 7.11(c)-(f). This is caused by the thermal stress induced by shrinkage of polymer due to cooling and solidification.

Stress distribution within the injection-molded polymer is induced not only by the deformation of polymer into the prescribed shape but also by the shrinkage of polymer due to cooling and/or solidification, and is affected by the viscoelasticity of polymer that is strongly dependent upon its temperature. In order to control the generation of molding defects due to deformation/residual-stress of the injection-molded polymer products, therefore, these factors must be taken into account comprehensively.

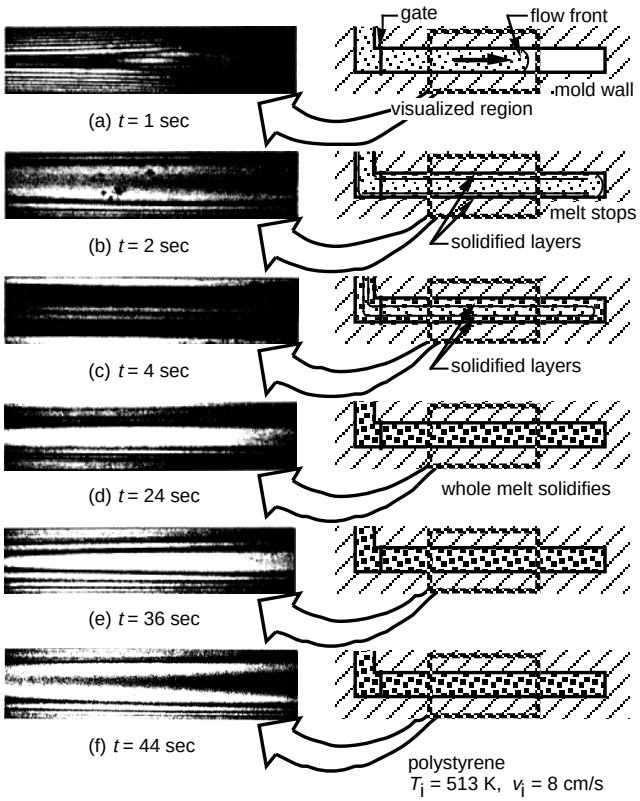

Figure 7.12 Birefringence observed in a polymer during the injection-molding process[4].

3. Measurement of Surface Deformation of the Injection-Molded Polymer

In general, it is believed that the surface shape of injection-molded polymer products is the transcription of the shape of mold, and thus the measurements of surface deformation occurring during the molding process have been seldom achieved so far. In order to examine the generation mechanism of molding defects related to the surface shape of the products, e.g. flow-mark introduced in the previous chapter, however, it is desirable to measure the surface deformation directly during the molding process.

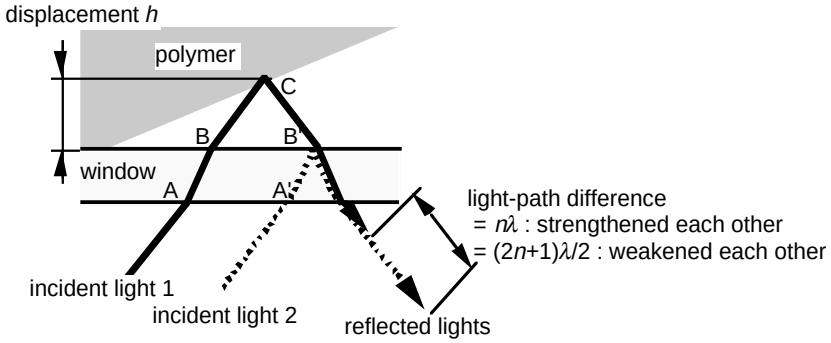

Figure 7.13 Optical interferometry for surface profile measurement.

Optical interferometry is often applied for high precision measurement of the surface shape or surface deformation of an object. In the optical infterferometry, the surface shape is measured by counting the number of fringes generated due to optical path difference between the light reflected from the object surface and that reflected from a standard (fixed) surface, and can be measured non-intrusively in the resolution of the order of wavelength of the light. Figure 7.13 shows the optical setup for applying this principle to the measurement of time-dependent surface deformation of an injection-molded polymer within the mold cavity during the molding process. A typical

result[5] is shown in Figure 7.14. This result is a snapshot of the generating flow-mark on an injection-molded polymer flowing in the mold cavity. As shown in this photo, whole the shape of flow-mark could not be measured, i.e. fringes due to the interference were countable only in limited regions where the polymer and the mold wall (window) were in contact with or close to each other, while a He-Ne laser which is a highly coherent light was used as the light source. This is explained by the fact that the size (depth) of the flow-mark is in the order of 0.1 mm or 1 mm, and is too much larger than the wavelength of light, 0.6 μm. This suggests that, in order to make an accurate measurement of surface shape/deformation, one should choice a measurement method having the resolution well matched with the scale of shape/deformation of the object.

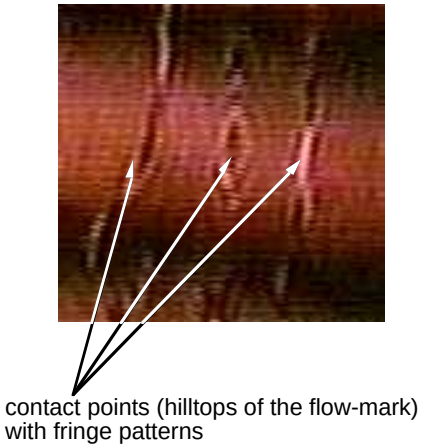

Figure 7.14 Surface profile of a flow-mark observed by the interferometry[5].

As a non-intrusive surface measurement technique having "lower" resolution, one can use so-called "moire topography." The moire topography visualizes the surface shape of the object as tha shape of fringes (moire fringes) induced by the light pattern projected onto the object surface, which deforms corresponding to the shape of the object surface, and a mask for generating the light pattern. Figure 7.15 shows a concept of the measurement of flow-mark generation applying the moire topography[6]. In this measurement, the light pattern, which was made by using a Michelson interferometer., was straight and parallel stripes, and thus the surface shape of the object can be evaluated by measuring the distortion of light stripes. Typical light pattern observed on the polymer surface is shown in Figure 7.16. One can see in this photo that the light stripes were deformed in wave-like curves according to the shape of flow-mark. By measuring the gap between the deformed light stripes and straight lines (original shape of the light stripes), surface shape of the object in depth direction can be evaluated non-intrusively. The maximum resolution of this method is several 10 μm, but this method can be applied for measuring the surface profiles of the scale of a several mm by adjusting the angle θ of incident light shown in Figure 7.15.

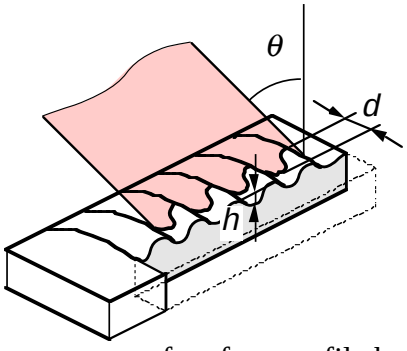

Figure 7.15 A concept of the measurement of surface profile by applying the moire topography.

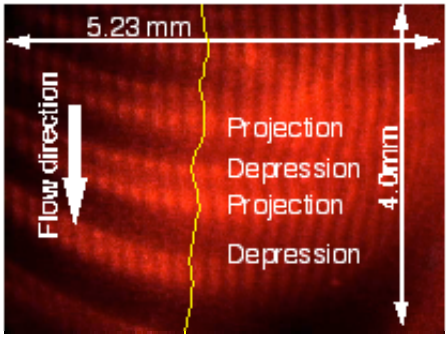

Figure 7.16 Surface profile of a flow-mark observed by the moire topography[6].

Figure 7.17 shows a typical result of this method. Time-dependent surface profiles of the flow-mark generating on an injection-molded polymer product are shown in this figure. Such a surface deformation of the injection-molded polymer products developing during the filling stage is mainly originated by the shrinkage of polymer in the surface layer due to cooling/solidification. Namely the deformations are dominated by the temperature distribution within the polymer during the filling stage, which is characterized by the combination of thermal properties of the polymer and the mold materials. Modeling of the surface deformation and the related heat transfer will be discussed in the next chapter in detail.

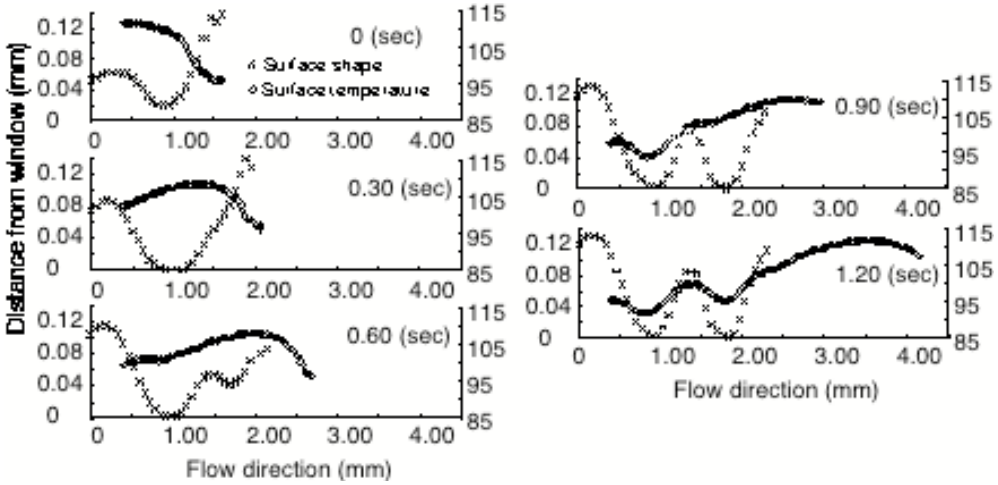

Figure 7.17 Surface profiles of the time-depended flow-mark generated on an injection-molded polymer product[6].

Problem

Devise a method, non-intrusive or intrusive, for measurement of surface profiles of the polymer during the injection-molding process other than those described above. Note that the polymer is in the mold cavity and its surface is soft until the whole polymer solidifies. Show the principle, and discuss the advantages and disadvantages of the method.

References

[3] Kurosaki, Y., Satoh, I. and Uchida, H.: Seikei-Kakou, 5-11 (1993) pp. 747-756.
[4] Kurosaki, Y., Satoh, I. and Ishii, K.: Trans. JSME, 56-522C (1990) pp. 504-511.
[5] Goto, K., Saito, T. and Satoh, I.: Seikei-Kakou '99 (Proc. 1999 Annual Meeting of JSPP), (1999) pp. 13-14.
[6] Torimura, S., Satoh, I. and Saito, T.: Seikei-Kakou '01 (Proc. 2001 Annual Meeting of JSPP), (2001) pp. 275-276.